

CURRENT – VOLTAGE STUDIES ON VACUUM EVAPORATED In₇₀Se₃₀ THIN FILMS

C. Viswanathan^a, G. G. Rusu^b, D. Mangalaraj^{a,c*}, Sa. K. Narayandass^a, J. Yi^c

^aThin film laboratory, Department of Physics, Bharathiar University, Coimbatore, India

^bSolid State Department, “Al. L. Cuza” University, Romania

^cSchool of Information and Communication Engineering, Sungkyunkwan University, Suwon Korea

In₇₀Se₃₀ thin films were deposited onto glass substrates at room temperature by thermal evaporation technique. The structure and surface morphology of the deposited films were investigated by X-ray diffraction (XRD) and Scanning Electron Microscopy (SEM). The composition of the InSe thin film was cross-verified with Rutherford Back Scattering (RBS) and Auger Electron Spectroscopy (AES). The electrical properties of the deposited films have been investigated for the temperature range from 130 to 350 K. Current – Voltage studies, at low voltages ($\leq 1 \times 10^5$ Vcm⁻¹) and low temperatures suggests that Mott’s Variable Range Hopping (VRH) conduction mechanism is dominant. The corresponding parameters were calculated. At higher voltages ($\geq 1 \times 10^5$ Vcm⁻¹) and higher temperatures, a region of space charge limited current (SCLC) conduction was observed. The analysis of I-V characteristics, based on SCLC measurements yields the following parameters: mobility (μ), trap filled level voltage (V_{TFL}), transition voltage (V_{tr}), trap concentration (N_t), density of states $N(E_F)$, trapping factor (θ). The transition from ohmic to square law behavior was used to calculate all of these parameters.

(Received August 18, 2004; accepted March 23, 2005)

Keywords: Indium selenide, Structural properties, Electrical properties

1. Introduction

Indium Selenide (InSe) belongs to III –VI compounds family being a layered semiconductor consisting of covalent bonded units (Se-In-In-Se) held together by Van der Waals forces and is one of the most suitable compound semiconductors for optoelectronic and photovoltaic applications [1]. To reduce the cost of the solar cells, several authors have studied thin films formed by starting from the material InSe [2]. These have typical characteristic of the layered semiconductors, namely: (A) – the low density of the dangling bonds on the surface because of the almost complete chemical bonds within the layer [3]; (B) – intercalation [4] and (C) – the mechanical weakness due to the weak Van der Waals forces between the layers. Property (A) makes it possible to form heterojunction devices with a low interface density of states. Property (B) allows altering the electrical properties of the semiconductors, which will be convenient in device processing. However, because of the disadvantage (C), it is almost impossible to form devices from layered semiconductor crystals. In order to overcome this disadvantage and to utilize the advantages (A) and (B), epitaxial films of layered semiconductors are needed. Although InSe thin films have been made by several methods, epitaxial films have not been reported. The large influence that the microstructure and secondary phases (surface layers) may have on the transport properties contribute further to the confusion.

It will be more convenient for the formation of well-oriented crystalline films if InSe films can be obtained by the vacuum evaporation technique [5]. To our knowledge there has been no report on transport mechanisms of In₇₀Se₃₀ thin films. The composition, structural, surface

* Corresponding author: dmraj800@yahoo.com

morphology and the nature of conduction mechanism both in low and high field at the temperatures ranging from 130 K to 350 K for $\text{In}_{70}\text{Se}_{30}$ thin films was observed for the present investigations.

2. Experimental

The In - Se alloy was prepared from its own constituent elements. Appropriate weight of indium and selenium (purity 99.999%, Nuclear Fuel Complex, Hyderabad) were mixed together and placed in a quartz tube, which is sealed under a vacuum of 10^{-5} Torr. The sealed quartz ampoule with the charge was placed in a rotating furnace at a temperature of 1073 K for 24 hours and then the compound was quenched into ice-water. $\text{In}_{70}\text{Se}_{30}$ thin films were deposited onto well-cleaned glass substrates held at room temperature using a conventional vacuum coating unit (12A4). Molybdenum boat was used as the source and the pressure inside the chamber was better than 10^{-5} Torr. The crystallinity was assessed with a Philips X-ray diffractometer. The thickness of the deposited films was calculated as 230 nm by using Multiple Beam Interference (MBI) technique. The composition of the film was also examined using Energy Dispersive Analysis of X-ray (EDAX), Rutherford Back Spectrometry (RBS) and Auger Electron Spectroscopy (AES). The Scanning Electron Microscopy (SEM) analysis was performed employing DSI 30 dual scan scanning electron microscope, a beam of very small diameter (~ 10 nm) is produced by electron gun and electron lenses. Films for I-V measurements were deposited onto glass substrates previously equipped with coplanar aluminum electrodes (Al /InSe /Al). All measurements were taken in the temperature range from 130 K to 350 K using standard techniques and automated systems.

3. Results and discussion

3.1. Structural characteristics of the films

Fig. 1 shows the XRD patterns for room temperature deposited InSe film. The films exhibit a diffraction pattern typical for a poly-hexagonal crystal structure [6]. The diffraction peak around $2\theta = 32.15^\circ$ corresponds to diffraction from the (006) plane. InSe crystallizes in the hexagonal system [6,7].

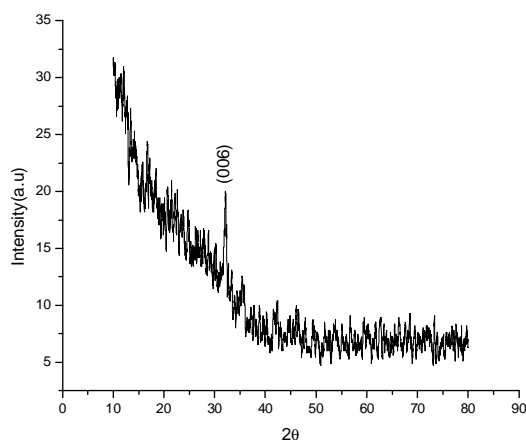


Fig. 1. Typical XRD spectra for studied samples.

From the XRD profiles, the crystallite size (D) of the films was calculated from the Debye Scherer's formula from the full-width at half-maximum (FWHM) β for the (006) plane. The strain is calculated from the slope of $\beta \cos \theta$ versus $\sin \theta$ plot using the relation

$$\beta = \frac{\lambda}{D \cos \theta} - \epsilon \tan \theta \quad , \quad (1)$$

where λ is wavelength of X ray and ϵ is microstrain.

The dislocation density (δ), defined as the length of dislocation lines per unit volume of the crystal has been calculated by using the formula $\delta = 1/D^2$. For the deposited film, the grain size, dislocation density and strain were calculated as 18.77 nm, 2.83×10^{15} lin/m² and 1.788×10^{-3} lin⁻² m⁻⁴ respectively.

3.2. Composition analysis

The Rutherford Back Scattering spectroscopy (RBS), Energy Dispersive Analysis by X-Ray (EDAX) (Fig. 2) and Auger Electron Spectroscopy (AES) spectrum reveal for Indium / Selenium at atomic percentage present in the deposited film the values of 68% / 32%, 70.55% / 29.45% and 71% / 29%, respectively.

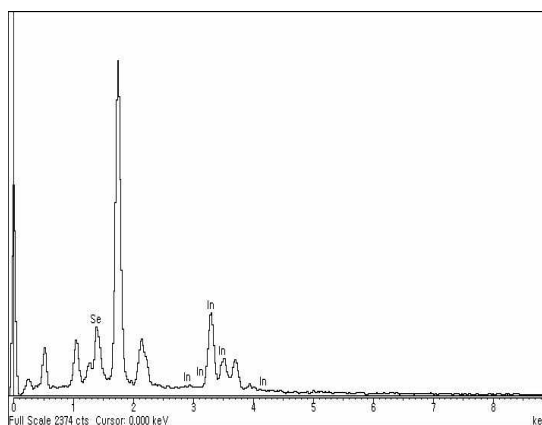


Fig. 2. EDAX spectra showing 70.55 and 29.45 atomic percents for In and Se respectively.

The surface analysis of the layers has been investigated visually by scanning electron microscopy. Fig. 3 shows the SEM images of polycrystalline InSe film grown onto glass substrates. The as deposited film shows crystalline nature with smaller grains [6, 7].

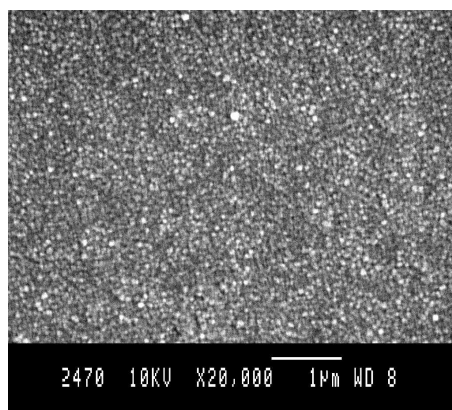


Fig. 3. SEM micrograph of the surface for room deposited samples.

3.3. Electrical properties (Low Field ($\leq 1 \times 10^5$ V cm⁻¹))

Localized states in a disordered material arises due to different types of defects such as impurities, connection tears, intrusions, lack of long range order, also depending upon the condition

under which the film is prepared. The charge transport takes place via phonon assisted hopping between localized states. Since the localized states have quantized energies extending over a certain range, activation energies is required for each hop. Hopping occurs either near the Fermi level or near the maximum of the density of the states. At lower temperatures, hopping dominates near the Fermi level. At higher temperatures, hopping dominates near the maximum of the density of states.

The investigations of the conduction mechanism of deposited films in the investigated temperature range (170-280 K) were made by assuming that at least one of the following three possible conduction mechanisms is dominant at respective temperature ranges (Fig. 4). They are: i) thermionic emission, in which $\sigma T^{1/2}$ varies exponentially with inverse temperature [8]; ii) tunneling for which σ varies as T^2 [9] and iii) variable range hopping in which $\ln(\sigma T^{1/2})$ depends on temperature as $T^{1/4}$ [10]. The temperature-dependent conductivity data were used to determine the temperature intervals over which one of the above theories was applicable. It was found that, under low field condition ($\leq 1 \times 10^5 \text{ Vcm}^{-1}$), for as deposited (230-280 K) films, the activation energy (E_σ) is 54 meV as calculated by the relation (2) where σ_0 is the pre-exponential factor (Fig. 5).

In the higher temperature region, the variation of conductivity with temperature for polycrystalline materials was found to obey Seto's [8] extended version of the Petritz model

$$\sigma\sqrt{T} = \sigma_0 \exp\left(\frac{-E_\sigma}{kT}\right) \quad , \quad (2)$$

E_σ being the activation energy of conductivity. In this model the trapped charges at grain boundaries produce carrier depletion and this is the main cause of grain boundary potentials. The height of the barrier at the grain boundaries and its temperature dependence has been examined by Gunal and Mamikoglu [11]. It was found that grains in the high temperature region are spatially depleted and the transport is mainly due to thermionic emission of carriers over the grain boundaries.

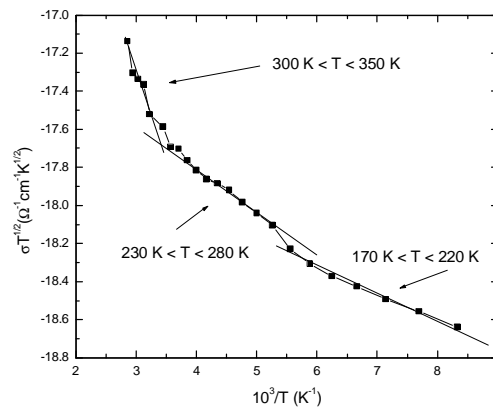


Fig .4. Dependence of $\sigma T^{1/2}$ vs. inverse temperature for full investigated temperature range.

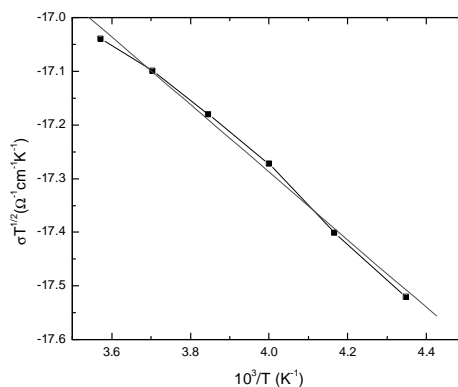


Fig. 5. Dependence of $\sigma T^{1/2}$ vs. inverse temperature in the range 230-280 K.

In the low temperature region, between 170 and 220 K, the observed conductivity – temperature dependence obey the variable range hopping theory established by Mott et al. [10]. A good fit of relation is given by [12]

$$\sigma\sqrt{T} = \sigma_0 \exp \left[- \left(\frac{T_0}{T} \right)^{1/4} \right] \quad (3)$$

In the present investigation under low temperature region the conduction mechanism may be the variable range hopping, since the plot of $\sigma T^{1/2}$ vs $T^{-1/4}$ fits well (Fig. 6).

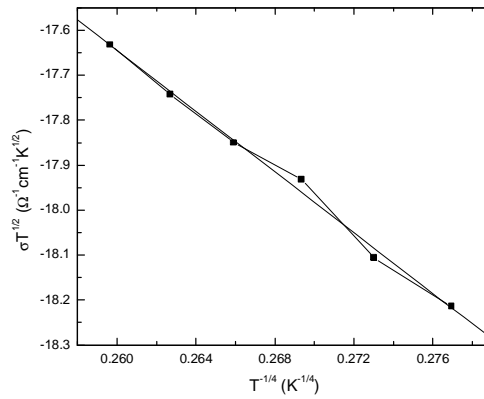


Fig. 6. Dependence of $\sigma T^{1/2}$ vs. $T^{-1/4}$ in the range 170 K ÷ 220 K.

From the slope and intercept, Mott's parameters such as degree of disorder T_0 , localized density of states $N(E_F)$, hopping range R_{hop} and average hopping energy W_{hop} , were evaluated (Table 1) using the expressions given by Paul and Mitra [12,13]. In these calculations, a typical phonon frequency of 10^{13} s^{-1} was assumed. The values of γR_{hop} and W_{hop} satisfy Mott's requirements ($\gamma R_{hop} > 1$ and $W_{hop} > kT$) for variable range hopping.

Table 1. The Mott parameters of InSe films.

In ₇₀ Se ₃₀ Films	Hopping dimension	Mott temp. T_0 (K)	$N(E_F)$ (cm ⁻³ eV ⁻¹)	R_{hop} (cm)	W_{hop} (meV)	E_σ (meV)
Poly-InSe	3D	1.30×10^6	1.803×10^{18}	1.50×10^{-8} at 200 K	154 at 200 K	54 (230-280 K)

3.4. Electrical properties (High Field ($\geq 1 \times 10^5 \text{ Vcm}^{-1}$))

The localized defect states in the forbidden gap can strongly influence the injected current as response to an applied voltage. Both the magnitudes of the current response and the actual form of the current density – voltage (I-V) characteristics are determined by the interaction of the carriers with such states. In fact, the charge is trapped at these localized defects and is immobilized. Therefore, due to the reduction of the current through trapping, the appearance of space-charge-limited current (SCLC) is inhibited until an adequately large field is applied. The transition from an ohmic region to an SCLC region depends markedly on the energy distribution of the trapping levels. Hence, there is a need for a systematic study of the transport properties of this material by a simple technique in view of its useful in energy-related applications [14].

For SCLC investigation, the I-V characteristic of the InSe films was measured at higher temperature regions. Here, the analysis of the experimental data was carried out according to the Lamberts model [15]. This method has been used to evaluate the electronic properties of high-resistivity materials. SCLC measurements were performed on amorphous InSe film in high electrical field ($\geq 1 \times 10^5 \text{ Vcm}^{-1}$) and for temperatures ranging from 300 K to 350 K. Typical SCLC characteristic at 340 K for InSe sample of thickness 230 nm are presented in Fig. 7. The curve shows a gradual transition from an ohmic region, where I is proportional to V , to a space-charge-trap-limited current region where I is proportional to V^n with $n > 2$. In the ohmic region the I-V dependence should be of the form [16]

$$I = Aq\mu_p p_0 \frac{V}{d} \quad (4)$$

where A is the electrode effective area of $4.2 \times 10^{-2} \text{ cm}^2$, q is the elementary charge, p_0 is the hole concentration, d is the sample thickness and μ_p is the hole mobility which can be found from the following equation [17]:

$$I = 6.510 \times 10^{11} \frac{AV^2 \mu_p T^{3/2}}{d^3 N_t} e^{-E_t/kT} \quad (5)$$

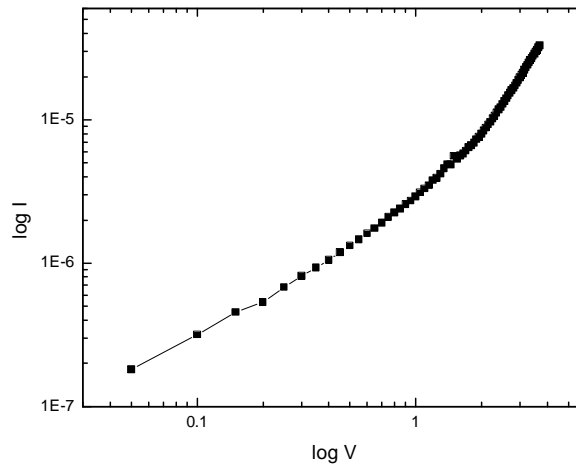


Fig. 7. Typical $\log(I)$ vs. $\log(V)$ curve for InSe film at 340 K.

Equation (5) predicts that in the square-law region, a plot of $\log_{10}(I)$ vs. T^{-1} [Fig. 8] should give a straight line summing that the $\mu_p T^{3/2}$ product is a weak temperature dependent factor. The current versus temperature data at a selected voltage are retrieved from the collected data. The mobility μ_p ($1.352 \times 10^{-11} \text{ cm}^2 \text{V}^{-1} \text{s}^{-1}$) can be determined from the slope and intercept of such plots by knowing the values of N_t and E_t . Using μ_p values, equation (4) yields p_0 and the effective mobility ($\mu_{\text{eff}} = \mu \theta$) was calculated. In the square law region, where I-V characteristic is controlled only by the shallow level, the current is given by [18]

$$I = \frac{9}{8} \frac{A \epsilon_s \mu_p \theta V^2}{d^3} \quad (6)$$

where ϵ_s is the static permittivity of the material and ($\theta = 0.47$) is the ratio of free to shallow trapped charge [19]. The steep rise in current preceded by the square law region occurs at

$$V_{TFL} = \frac{qN_t d^2}{2\epsilon_s} \quad (7)$$

where V_{TFL} is the trap-filled limited voltage, estimated as 3.1 V.

For a single level of shallow traps, whose density is N_t , the dominant trap level ($E_t - E_v$) above the valence band edge is calculated from the relation [20]

$$\theta = \left(\frac{N_v}{N_t} \right) \exp\left(\frac{-(E_t - E_v)}{kT} \right) \quad , \quad (8)$$

where $N_v = 2(2\pi m^* kT/h^2)^{3/2}$ is the effective density of states at the valence band edge.

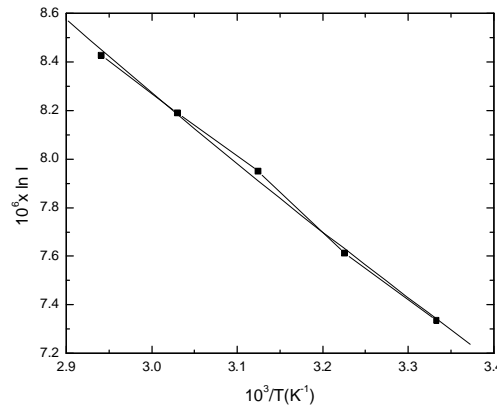


Fig. 8. Temperature dependence of current at a constant bias of 2 V for InSe film.

The value of N_v ($=1.0689 \times 10^{19} \text{ cm}^{-3}$) was calculated by taking $m^*=0.5$ m[21] and $T = 340$ K. According to Lampert's theory, the I-V characteristic consists of an ohmic region at low voltages, followed by a super linear region in which the current density expression holds the expression

$$I \propto \frac{V^{l+1}}{d^{2l+1}} \quad , \quad (9)$$

where $l+1=n$ is known as power law gradient and l is equal to the ratio T_v/T , T is the absolute temperature and T_v is a temperature characterizing the exponential trap distribution $N(E)$ described by

$$N(E) = N_0 \exp\left(-\frac{E}{kT_v} \right) \quad , \quad (10)$$

where N_0 is the value of $N(E)$ at the valence band edge. The total concentration of traps, N_t , is the integral over the exponential distribution $N(E)$, and is given by the relation [22]

$$N_t = N_0 kT_v \quad . \quad (11)$$

The transition voltage V_{tr} is given by [23]

$$V_{tr} = \left(\frac{p_0}{N_c} \right)^{1/l} \frac{d^2 q N_0 kT_v}{\epsilon_s} \quad . \quad (12)$$

The gradient in the SCLC region is 2.45, suggesting an exponential trap distribution. Using these gradients, T_v was determined as 493 K. From T_v , V_{tr} , and the earlier p_0 , the values N_0 ($5.318 \times 10^{19} \text{ cm}^{-3} \text{ eV}^{-1}$) is evaluated from equation (8) and are tabulated in Table 2. The total

concentration of traps (N_t) in the exponential distribution is obtained from equation (7) as $2.261 \times 10^{18} \text{ cm}^{-3}$ for InSe thin films.

Table 2. Transport parameters of InSe films.

InSe Films	μ ($\text{cm}^2 \text{ V}^{-1} \text{ s}^{-1}$)	V_{TFL} (V)	θ	N_t (cm^{-3})	$N(E)$ ($\text{cm}^{-3} \text{ eV}^{-1}$)
Poly InSe	1.352×10^{-11}	3.1	0.47	2.261×10^{18}	5.318×10^{19}

4. Conclusions

The prepared InSe film shows polycrystalline in nature and is confirmed by SEM observations. The composition of the prepared film is confirmed by XPS and EDAX spectrum. In DC conduction, at low field, up to the temperature 220 K, the conduction mechanism of Mott's variable range hopping is dominant and necessary parameters are calculated. Above 230 K, thermionic emission conduction mechanism is observed. At higher voltage and temperature, the SCLC region was observed.

Acknowledgement

One of the authors, C. Viswanathan, acknowledges the University Grants Commission, New Delhi under research grant F.No.10-65/2001 (SR-1) for the award of a Project Fellow.

References

- [1] Y. Hasegawa, Y. Abe, Phys.Stat. Sol. A, **79**, 615 (1982).
- [2] J. C. Bernede, S. Marsilact, A. Conan, A. Godoy, J. Phys: Cond. Matter **8**, 3439 (1996).
- [3] J. V. McCany, R. B. Murry, J. Phys. C. **10**, 1211 (1977).
- [4] B. Fotouhi, O. Gorochov, A. Katty, N. Le Nagard, C. Levy-Clement, D. Schleich, B. Theys, H. Tributsch, Sci. Energy Res. Dev. Eur. Community, Ser.D, **2**,78 (1983).
- [5] M. Yudasaka, K. Nakanishi, Thin Solid Films **156**, 145 (1988).
- [6] Jin-Ho Park, Mohammad A. Fzaal, Madeleine Melliwell, Mohmmad, A. Malik, Paul O'Brien Jim Raftery, Chem.Mater. **15**, 4205 (2003).
- [7] In-Hwan Choi, Peter Y. Yu, J. Appl. Phys. **93**(8), (2003).
- [8] J. Y. W. Seto, J. Appl. Phys. **46**, 5247 (1975).
- [9] M. V. Garcia-Cuenca, J. L. Morenza, J. Esteve, J. Appl. Phys. **56**, 1738 (1984).
- [10] N. F. Mott, E. A. Davis, Electronics Process in Non-Crystalline Materials Clarendon Press, Oxford (1979).
- [11] I. Gunal, H. Mamikoglu, Thin Solid Films, **185**, 1 (1990).
- [12] D. K. Paul, S. S. Mitra, Phys. Rev. Lett. **31**, 1000 (1973).
- [13] M. Thamilselvan, K. Premnazer, D. Mangalaraj, Sa. K. Narayandass, Physica B **337**, 404 (2003).
- [14] S. M. El-Sayed, Vacuum **65**, 177 (2002).
- [15] M. A. Lampert, P. Mark, Current Injection in Solids, Academic Press, New York, (1970).
- [16] R. D. Gould, Thin Solid Films **125**, 63 (1985).
- [17] A. E. Rakhshani, J. Appl. Phys. **69**(4), 2365 (1991).
- [18] T. G. Abdel-Malik, Int. J. Electron **72**(3), 409 (1992).
- [19] M. A. Lampert, Rep. Prog. Phys. **27**, 329 (1964).
- [20] A. Rose, J. Phys. Rev. **97**, 1538 (1955).
- [21] C. T. Iynch, Practical Handbook of Materials Science, CRC, Bocaaton, (1989).
- [22] R. D. Gould, M. S. Rahman, J. Phys. D **14**, 79 (1981).
- [23] R. D. Gould, B. A. Carter, J. Phys. D, **16**, 1201 (1983).